

How Tongxie-Yaofang Regulates Intestinal Synaptic Plasticity by Activating Enteric Glial Cells and NGF/TrkA Pathway in Diarrhea-Predominant Irritable Bowel Syndrome Rats

Xiaofang Lu, Shengsheng Zhang

Center of Digestive, Beijing Hospital of Traditional Chinese Medicine, Capital Medical University, Beijing, People's Republic of China

Correspondence: Shengsheng Zhang, Center of Digestive, Beijing Hospital of Traditional Chinese Medicine, Capital Medical University, Beijing, People's Republic of China, Tel/Fax +86-10-87906634, Email zhangshengsheng@bjzhongyi.com

Purpose: Diarrhea-predominant irritable bowel syndrome (D-IBS) is a frequent functional gastrointestinal disease that affects health and quality of life owing to its high incidence and recurrence rate. Tongxie-Yaofang (TXYF) is a traditional Chinese medicine prescribed for D-IBS. However, the therapeutic mechanism of TXYF has not been fully elucidated. This study aimed to investigate the effects of TXYF on visceral hypersensitivity in stress-induced D-IBS rats and the underlying mechanisms.

Methods: Electromyographic (EMG) activity of the external oblique muscles and the abdominal withdrawal reflex (AWR) score captured by Barostat were used to quantify the effect of TXYF on visceral sensitivity. Transmission electron microscopy (TEM) was used to observe the ultrastructure of the enteric nervous system (ENS). For molecular detection, the colonic expression of enteric glial cell's (EGC's) activation markers, glial fibrillary acidic protein (GFAP) and calcium-binding protein S100 β , NGF, TrkA, synaptic plasticity-related factors, synaptophysin (SYN) and postsynaptic density-95 (PSD-95), glutamate, glutamate receptors α -amino-3-hydroxy-5-methyl-4-isoxazole-propionic acid receptor (AMPA), and N-methyl-D-aspartate receptor (NMDAR) were detected by immunohistochemistry, enzyme-linked immunosorbent assay, and real-time PCR. An ex vivo experiment was conducted to measure the EGC-induced NGF release.

Results: TXYF decreased the EMG activity and AWR scores in rats with D-IBS. Under TEM, TXYF improved the dense and irregular nerve arrangement, narrowed the synaptic cleft, and decreased the number of synaptic vesicles in D-IBS rats. In addition, TXYF decreased the expression of GFAP, S100 β , SYN, and PSD-95; down-regulated the levels of NGF, TrkA, and glutamate; and reduced the mRNA expression of AMPAR1, NMDAR1, and NMDAR2B. In an ex vivo experiment, TXYF decreased NGF release in D-IBS rats, and this trend disappeared under EGC inhibition.

Conclusion: TXYF alleviated visceral hypersensitivity in D-IBS rats possibly by improving synaptic plasticity through inhibiting the activity of EGCs and the NGF/TrkA signaling pathway in the colon.

Keywords: diarrhea-predominant irritable bowel syndrome, Tongxie-Yaofang, visceral hypersensitivity, synaptic plasticity, enteric glial cell

Introduction

Diarrhea-predominant irritable bowel syndrome (D-IBS) as one of the most important clinical subtypes of irritable bowel syndrome (IBS) is characterized by diarrhea and abdominal pain in the absence of other diseases to cause these symptoms.¹ Epidemiological surveys have shown that D-IBS has a high worldwide incidence. A systematic review and meta-analysis reported that the pooled prevalence of IBS in 53 studies was 9.2% using Rome III criteria, the pooled prevalence of IBS in 6 studies was 3.8% using Rome IV criteria, and IBS-D was the most common subtype, accounting for 31.5%.² A recent epidemiological investigation including 73,076 adult respondents from 33 countries in 6 continents showed that the prevalence of D-IBS was 1.2%.³ In China, the prevalence of IBS among adults could be approximately 5–10%.⁴ The high prevalence rate has a negative impact on patients' quality of life and medical resources. At present, the

treatment methods of D-IBS are constantly updated and have shown a certain efficacy in clinical practice, however, it should not be ignored that the modern treatment of D-IBS has a high recurrence rate and poor comprehensiveness.⁵ Adapted to clinical demand, traditional Chinese medicine (TCM) syndrome differentiation has gradually shown its advantages.

D-IBS corresponds to TCM diseases “diarrhea” and “abdominal pain”, whose basic pathogenesis is “liver depression and spleen deficiency”. Tongxie-Yaofang (TXYF) is the recommended prescription for D-IBS.⁶ Evidence-based medical evidence has shown that TXYF can relieve symptoms and improve quality of life in D-IBS,⁷ but because its therapeutic mechanism is not fully understood, its international application has certain limitations.

Current evidence has confirmed that the pathogenesis of D-IBS includes disturbances in intestinal motility, visceral sensitivity, secretion, immunity, and microecosystems, among which intestinal hypersensitivity was one of the research focuses.⁸ In a previous study, it was confirmed that TXYF could alleviate visceral hypersensitivity in D-IBS,⁹ but the regulatory mechanisms underlying visceral hypersensitivity have not been clarified. It has been well known that intestinal sensation is inseparable from the local regulation of the enteric nervous system (ENS). Synapse, as an essential unit of the ENS, plays a key role in the regulation of neural activity, and synaptic plasticity has been demonstrated to be involved in intestinal hypersensitivity.¹⁰ Besides, previous pathophysiological studies have shown that the activation of enteric glial cells (EGCs) and its released neurotrophic factors (NGF) participate in the process of synaptic plasticity and visceral pain.^{11,12}

Therefore, this study aimed to explore the mechanism by which TXYF regulates visceral sensitivity, which may be related to synaptic plasticity mediated by EGC activation and the NGF signaling pathway.

Materials and Methods

Animals

Male Sprague-Dawley rats (one-day-old) were obtained from SPF Biotechnology Co., Ltd., Beijing, China (Certification no. SCXK (Jing) 2019–0010) and maintained at the Beijing Institute of Traditional Chinese Medicine. All the rats had free access to water and food and kept under a 12-hour light/dark cycle (lights on at 08:00) at 20–26 °C and 40–70% relative humidity. All experiments were performed with approval from the Animal Ethics Committee of the Beijing Institute of Traditional Chinese Medicine (permit No.2020120103). The animal care and treatment was in accordance with the Guide for the Care and Use of Laboratory Animals issued by National Institutes of Health.

Protocol

Sixty-nine rats were included in the experiment and all the rats were randomly assigned to three groups using a random number table method: 1) Normal group (twenty-three rats): no neonatal maternal separation (NMS) and no restraint stress (RS); 2) D-IBS group (twenty-three rats): NMS and RS; and 3) TXYF group (twenty-three rats): NMS and RS followed by TXYF intervention. NMS was conducted during postnatal days (PNDs) 2–21, and RS was conducted during PNDs 50–59. From PNDs 60 to 74, rats in the TXYF group were intragastrically administered TXYF. After drug intervention, six rats in each group were arranged for the detection of visceral sensitivity, colonic tissues were provided by six rats in each group for real-time PCR and enzyme-linked immunosorbent assay (ELISA), and colonic specimens were extracted from five rats in each group for immunohistochemistry and transmission electron microscope observation. The remaining six rats in each group were used in an ex vivo experiment to detect NGF release. The sample size in each experimental unit was decided based on “Resource Equation Approach” published by Arifin et al in 2017.¹³ The ARRIVE guidelines (Animal Research: Reporting of In Vivo Experiments) 2.0 was used to assess the quality of the experiment.¹⁴ The experimental process is illustrated in [Figure 1](#).

Neonatal Maternal Separation and Restraint Stress

The D-IBS model was induced by a combination of neonatal maternal separation (NMS) and restraint stress (RS).^{15,16} On PNDs 2–21, from 8:00 a.m. to 11:00 a.m., the infant rats were separated from the maternal rats and placed into individual compartments at a constant temperature 23 ± 0.5 °C. Three hours later, the litter was immediately returned to maternity

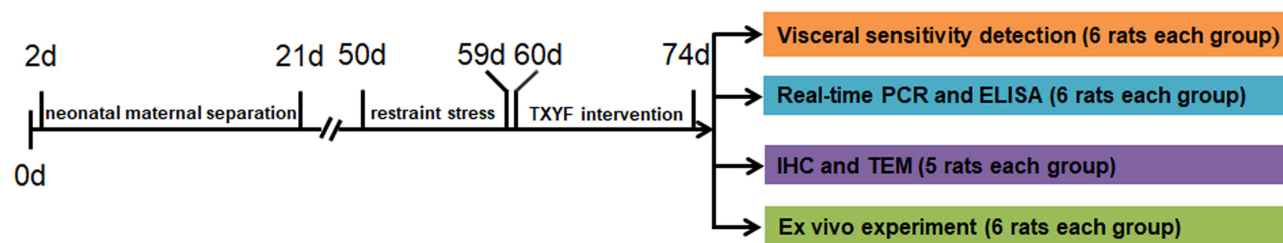


Figure 1 Experimental design. The neonatal maternal separation and restraint stress were conducted respectively during postnatal days 2 to 21 and 50 to 59. From postnatal days 60 to 74, the rats in TXYF group were given TXYF formula. After drug intervention, the rats were arranged for the detection of visceral sensitivity and ex vivo experiment. And the colonic tissues were obtained from the post-intervention rats for real-time PCR, enzyme-linked immunosorbent assay (ELISA), immunohistochemistry (IHC) and transmission electron microscope (TEM) detection.

Abbreviations: ELISA, enzyme-linked immunosorbent assay; IHC, immunohistochemistry; TEM, transmission electron microscope.

cages. On PNDs 50–59, the rats were placed into a restraint device for 2 h (between 8:00 a.m. and 10:00 a.m.), which only limited lateral movement without any dyspnea.

TXYF Composition and Administration

The TXYF formula comprised four Chinese herbal medicines: Rhizoma Atractylodis Macrocephalae, Radix Paeoniae Alba, Pericarpium Citri Reticulatae and Radix Saposhnikoviae, whose proportions of raw components were 6:4:3:2 according to the records in Danxi Xinfā. All ingredients of TXYF used in our study were obtained from the herbal pharmacy in Beijing Hospital of Traditional Chinese Medicine affiliated to Capital Medical University (Beijing, China). The crude drugs were soaked for 2h and boiled twice in distilled water, first for 30 min and then for 20 min. Ultimately, a concentration of 2.46 g/mL medicinal liquid was obtained. The TXYF group was administered TXYF formula (2 mL/100 g bodyweight/day) twice daily by gavage, and the Normal and D-IBS groups were treated with the same volume of distilled water for 14 consecutive days.

Pharmaceutical Component Analysis of TXYF by Ultra Performance Liquid Chromatography-Tandem Mass Spectrometry (UPLC-MS/MS)

Chromatographic separation of the components in TXYF was done by a Dionex UltiMate™ 3000 ultra performance liquid chromatography system (Thermo Fisher Scientific Inc., Waltham, Massachusetts, USA) and achieved by Waters ACQUITY UPLC HSS T3 column (1.8 μ m, 100 mm \times 2.1 mm) (Waters Corporation, Milford, Massachusetts, USA) at a temperature of 40 °C and a flow-velocity of 0.3 mL/min. Mass spectrometry was performed using a quadrupole orbital ion-trap mass spectrometer (Thermo Fisher Scientific Inc., Waltham, Massachusetts, USA). The voltages of the positive and negative ion source were 3.7 kV and 3.5 kV respectively, capillary heating temperature was 320 °C and the solvent heating evaporation temperature was 300 °C. All data were collected using Xcalibur 2.2 SP 1.48 software (Thermo Fisher Scientific Inc., Waltham, Massachusetts, USA).

Visceral Sensitivity to Graded Colorectal Distention (CRD)

Visceral sensitivity to colorectal distention (CRD) was quantified by electromyographic (EMG) activity of the external oblique muscles and the abdominal withdrawal reflex (AWR) score as described previously.¹⁷ After 14-days of pharmacological intervention, the rats were anesthetized with 2% isoflurane and a pair of silver electrodes was implanted in the external oblique muscle for subsequent performance. A 5 cm-long flexible balloon attached to the tygon tubing was inserted through the anus, positioned 2 cm from the anal verge, and fixed onto the base of the tail. Rats were housed in small cages. After the rats woke up, the EMG signal was recorded using a Power Lab system (AD instrument Co., Ltd., New South Wales, Australia) under the CRD with 30s of distention (20, 40, 60, and 80 mmHg), followed by a 3-min rest conducted using a barostat (G&J Electronics Co., Ltd., Toronto, Ontario, Canada). The EMG activity was calculated as the ratio of the area under the curve (AUC) during CRD (30 s) to the AUC before CRD (30 s). Visual observation of the AWR was used to measure behavioral responses to CRD by a blinded observer. The AWR score was measured as follows: 0, normal behavior without response; 1, slight head twist; 2, abdominal muscle contraction; 3, abdominal wall lifting; 4, body arching and lifting of the pelvic structures.

Sample Collection

Distal colonic tissues (approximately 6–7 cm from the anus) were obtained from all three groups. 2 cm fresh tissue was stored at -80°C for the measurement of ELISA, real-time PCR. Colonic tissue (0.5 cm) was fixed in a 4% paraformaldehyde solution for more than 24 h. After dehydration and transparency, the tissues were embedded in paraffin and sliced continuously at $3\ \mu\text{m}$ for immunohistochemical staining. Colonic tissue (0.5 cm) was added to the fixation solution for ultrastructural observation.

Immunohistochemistry

The $3\ \mu\text{m}$ colonic tissue slices were conducted as follow: 1) used xylene and gradient alcohol for paraffin depletion and rehydration, then used the distilled water to wash; 2) added EDTA antigen repair buffer (pH 9.0) to repair the tissues, then recovered to room temperature and rinsed with PBS for $5\ \text{min} \times 3$; 3) added 3% hydrogen peroxide solution onto the tissues to eliminate endogenous peroxides and incubated them at room temperature for 25 min in the wet box away from light, then rinsed with PBS for $5\ \text{min} \times 3$; 4) added BSA to seal the tissues and incubated them at room temperature for 30 min in the wet box; 5) added the primary antibody (GFAP: 1:2000, GB11096; S100 β : 1:2000, GB11359; SYN: 1:3000, GB112945; PSD-95: 1:200, GB11277; Servicebio technology Co., Ltd., Wuhan, China) and incubated overnight at 4°C ; 6) the next day, the tissues were retemperated for 30 min and washed with PBS for $5\ \text{min} \times 3$; 7) added secondary antibodies (HRP conjugated goat anti-rabbit IgG (H+L): 1:200, GB23303, Servicebio technology Co., Ltd., Wuhan, China) and incubated at room temperature for 50 min, and rinsed with PBS for $5\ \text{min} \times 3$ times; 8) DAB color rendering which was controlled under the microscope and terminated by tap water; 9) hematoxylin was re-dyed for 3 min, and after being dehydrated and transparent, the slices were sealed with neutral gum.

Positive cells were stained brown or tan. At $20\times$ magnification, five visual fields with dense positive particles were randomly selected for each specimen and five specimens were included in the final analysis. Image-Pro Plus (Vision 6.0) software was used to calculate the integrated optical density (IOD) of each field and the average IOD of each specimen was calculated.¹⁸

Ultrastructure Observation

The obtained colon tissues were trimmed into 1 cubic millimeter tissue blocks which were fixed with a buffer solution of 2.5% glutaraldehyde phosphate for more than 2 h and 1% osmic acid for 2 h. Successively use 50%, 70%, 90% ethanol, 90% ethanol and acetone, 90% acetone, and 100% acetone for dehydration. Pure acetone and overnight embedding solutions were used before the tissue blocks were sliced continuously at 70 nm and double-stained with 2% uranium acetate-lead citrate. The ultrastructure of the ENS was observed and filmed by transmission electron microscope HT7800 (80KV) (Hitachi, Ltd., Tokyo, Japan).

ELISA

After lysis in lysis buffer, colonic samples were centrifuged at 5000 rpm for 15 min. The supernatants were collected for measurement. The levels of NGF, TrkA, and glutamate were determined by ELISA according to the manufacturer's instructions (NGF, E02N0014; TrkA, E02N0676; glutamate, E02G0401, Blue Gene Technology Co., Ltd., Beijing, China).

Real-Time PCR

Total RNA was extracted from colonic tissue using TRIZOL extraction reagent (Invitrogen Co., Ltd., Carlsbad, California, USA). A volume of $20\ \mu\text{L}$ cDNA reaction recipe involved template RNA $1.0\ \mu\text{g}$, reverse transcription primer T18 $1.0\ \mu\text{L}$, 10 mM dNTPs $1.0\ \mu\text{L}$, RNase Inhibitor $0.5\ \mu\text{L}$, M-MLV Rtase $1.0\ \mu\text{L}$ and the remainder was DEPC. The $10\ \mu\text{L}$ products for qPCR were made in a reaction system containing cDNA template $1.0\ \mu\text{L}$, primer F/R $0.3\ \mu\text{L}$, TB Green[®] Premix Ex Taq[™] II $5\ \mu\text{L}$ and the remainder was ddH₂O. Gene-specific primers were designed for each of the target genes. Real-time quantitative PCR was performed using a Roche LightCycler[®] 480II real-time PCR instrument (Roche Co., Ltd., Basel, Switzerland). Detection conditions were: 95°C for 5 min; 40 cycles of 95°C for 10s and 60°C for 30s. β -actin was used as an internal control to normalize the expression of all other genes. The $2^{-\Delta\Delta\text{Ct}}$ method was used to analyze relative changes in gene expression. The following primers were used: AMPAR1, F: GCTGGTGGTGGTTGACTGTGAAT and R: TGGC

TCCGCTCTCCTGAACTTA; NMDAR1, F: GTGGTGGCACAGGCAGTTCA and R: GTCACTCCGTCCGCAT ACTTAGAA; NMDAR2B, F: GTGCTCAACTACATGGCTGGAAGG and R: GCTGGCTGCTCATCACCTCATTC; β -actin, F: GAAGTGTGACGTTGACATCCG and R: GAAGTGTGACGTTGACATCCG.

NGF Release

Spontaneous NGF released by the colonic segments was evaluated using a previously described method.¹⁹ 150 mg of colonic segment from each rat were equilibrated in 1 mL Krebs-Henseleit solution (K-HS) gassed with 95% O₂ and 5% CO₂ and maintained at 37 °C for 30 min. The tissues were then incubated with the vehicle (K-HS) or DL-fluorocitrate (100 μ M, F9634, Sigma Co., Ltd., Taufkirchen, Germany) for 30 min. The collected supernatants were frozen at -20 °C for NGF level measurement by ELISA according the NGF kit (E02N0014, Blue Gene Technology Co., Ltd., Beijing, China). The experimental process is illustrated in Figure 2.

DL-fluorocitrate was prepared as described in a previous study.²⁰ DL-fluorocitrate barium was dissolved in distilled water to obtain a clear solution. Sodium sulfate was then added to the clear solution to precipitate the barium. This solution was then filtered through a 0.2 μ m filter, and distilled water was added to make up the final volume. The preparation of K-HS: NaCl 117 mmol/L, KCl 4.7 mmol/L, MgCl₂ 1.2 mmol/L, NaHCO₃ 24.8 mmol/L, KH₂PO₄ 1.2 mmol/L, CaCl₂ 2.56 mmol/L, and glucose 11.1 mmol/L.

Statistical Analysis

Statistical software (SPSS 17.0) was used to analyze all data. First, normality and homogeneity of variance were tested. For the normality test, Q-Q plots were conducted. When the data conformed to normal distribution and equal variance ($P > 0.05$), one-way analysis of variance (ANOVA) was used for comparisons among groups, and the least significant difference (LSD) test was used for comparisons between two groups. The measurement data were expressed as mean \pm SEM. $P < 0.05$ was considered statistically significant.

Results

Pharmaceutical Components of TXYF

The major components of TXYF are shown in the base peak intensity (BPI) chromatograms of the positive and negative ions in Figure 3. A total of 81 ingredients were detected, of which 11 were from Rhizoma Atractylodis Macrocephalae,

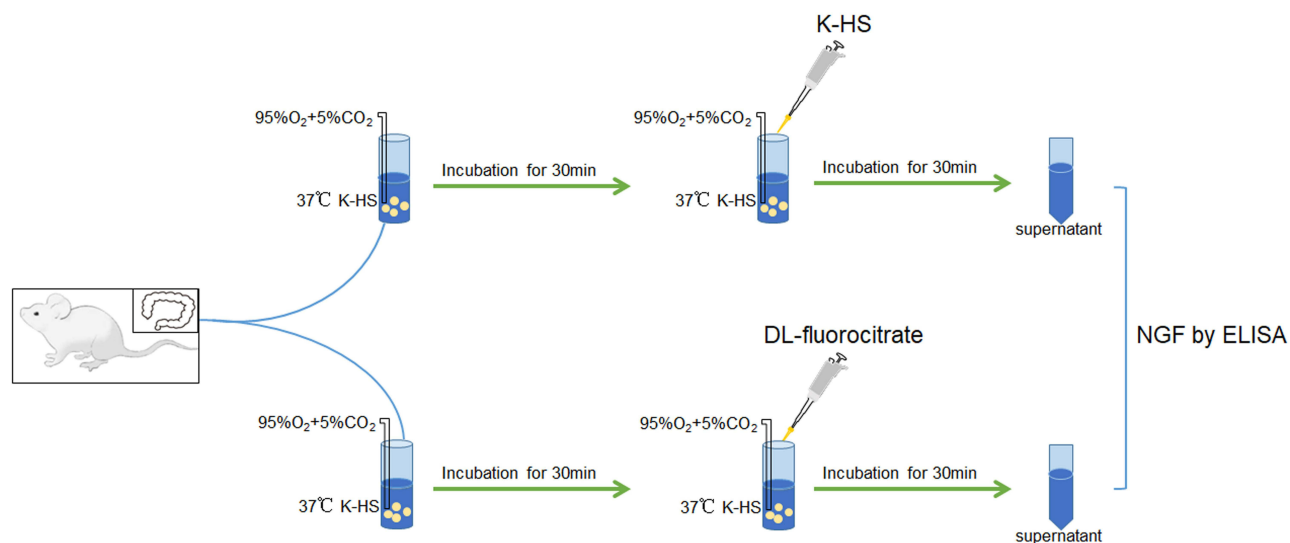


Figure 2 Procedure of ex vivo experiment. The NGF release detection was conducted by the ex vivo experiment. The colonic segments from the three groups were incubated in Krebs-Henseleit's solution (K-HS) for 30 min, next the tissues were incubated with vehicle (K-HS) or DL-fluorocitrate for 30 min. Then the supernatants were collected for NGF level measurement. The experimental environment was maintained at 37°C and gassed with 95%O₂ and 5%CO₂.

Abbreviations: K-HS, Krebs-Henseleit's solution; NGF, nerve growth factor; ELISA, enzyme-linked immunosorbent assay.

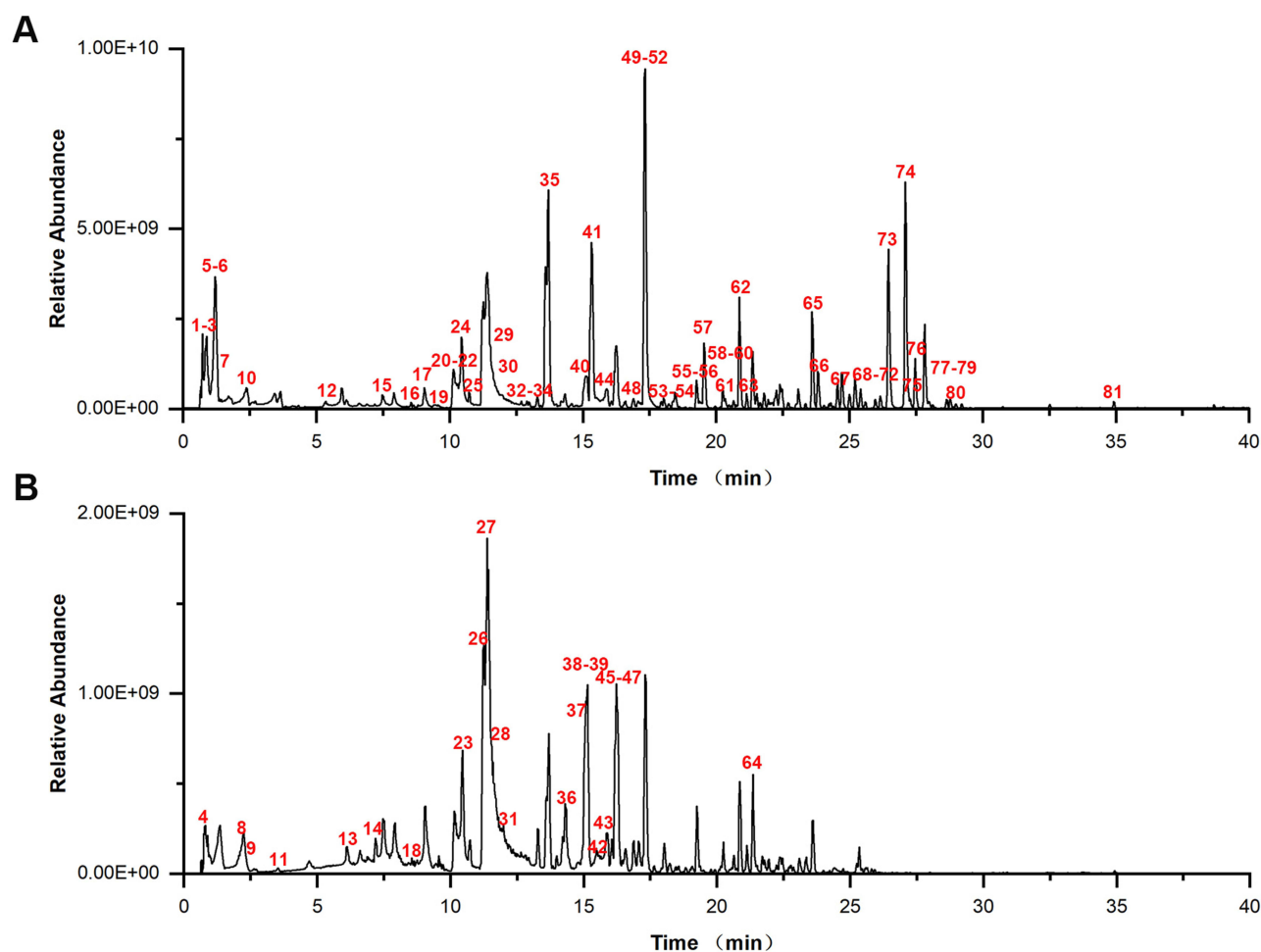


Figure 3 Major components of TXYF formula detected by UPLC-MS/MS. **(A)** Positive ion chromatogram, **(B)** negative ion chromatogram.
Abbreviation: UPLC-MS/MS, ultra performance liquid chromatography-tandem mass spectrometry.

24 active compounds were from *Radix Paeoniae Alba*, 22 active compounds were from *Pericarpium Citri Reticulatae*, and 31 active compounds were from *Radix Saposhnikovia*.

Effect of TXYF on the Visceral Sensitivity

A graded AWR response to CRD was scored for the rats. The D-IBS group had higher AWR scores than the Normal group (60 mmHg: LSD test, $P=0.036$; 80 mmHg: LSD test, $P=0.013$). After treatment with TXYF, the AWR score significantly decreased in the TXYF group compared with that in the D-IBS group (60 mmHg: LSD test, $P=0.008$; 80 mmHg: LSD test, $P=0.029$) (Figure 4A). EMG was recorded in response to the graded intensity of the CRD, at the same time, AWR response was scored. The D-IBS group exhibited a higher EMG AUC than the Normal group (40 mmHg: LSD test, $P=0.003$; 60 mmHg: LSD test, $P=0.003$; 80 mmHg: LSD test, $P=0.000$). After treatment with TXYF, the EMG AUC significantly decreased in the TXYF group compared with that in the D-IBS group (40 mmHg: LSD test, $P=0.039$; 60 mmHg: LSD test, $P=0.021$; 80 mmHg: LSD test, $P=0.001$) (Figure 4B). Typical EMGs are shown in Figure 4C.

Effect of TXYF on the EGC Activity

Glial fibrillary acidic protein (GFAP) and calcium-binding protein S100 β are expressed in activated EGCs. Images of GFAP (Figure 5A) and S100 β (Figure 5B) under a light microscope in the Normal, D-IBS, and TXYF groups are shown. Strong positive expressions of GFAP and S100 β were observed mainly in the myenteric plexus, and a small amount of expression was also found in the submucosal plexus. The D-IBS group showed increased IOD compared to the Normal

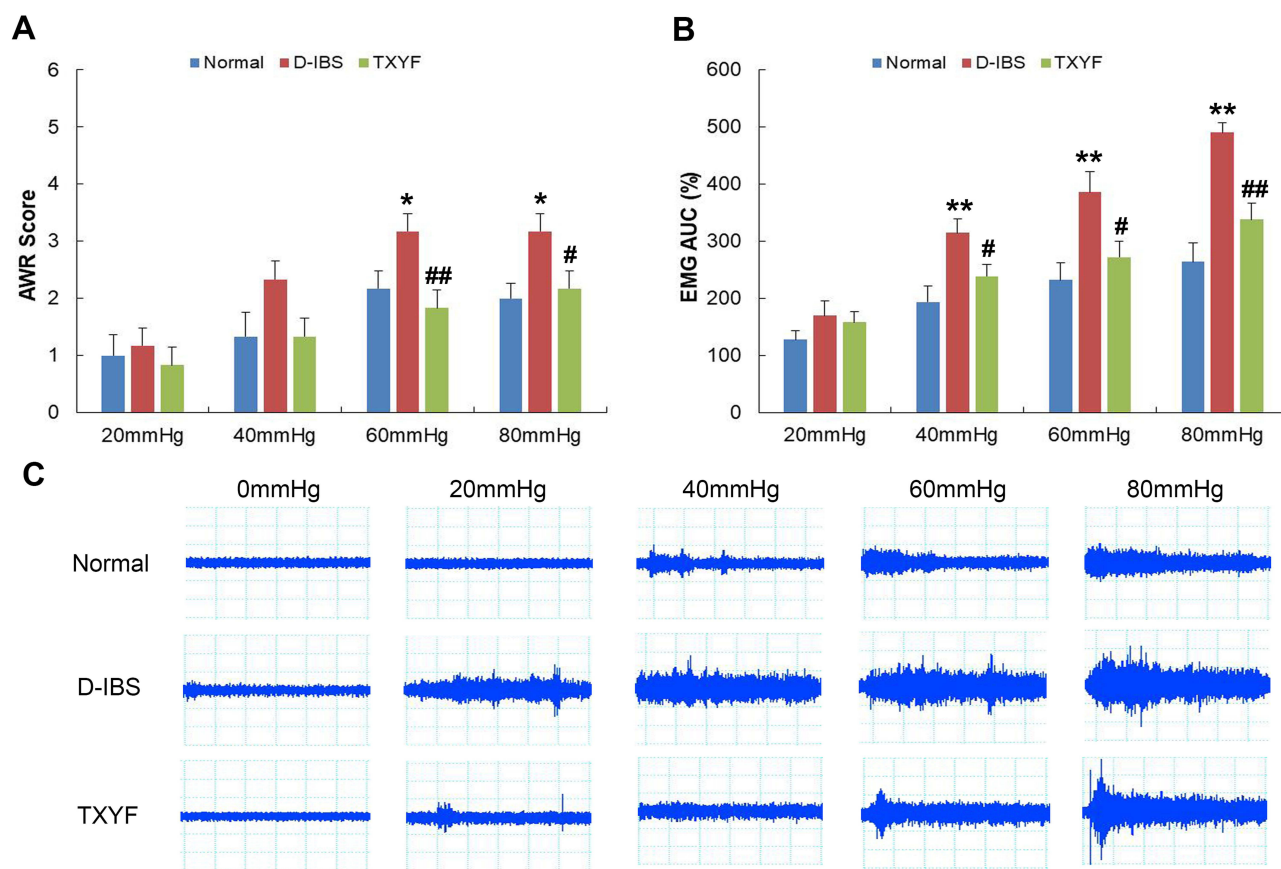


Figure 4 Effect of TXYF on colonic sensitivity in D-IBS rats. **(A)** Abdominal withdrawal reflex (AWR) score and **(B)** area under the curve (AUC) of electromyography (EMG) in response to graded distension pressure were measured to evaluate the colonic sensitivity. **(C)** Typical images of EMG activity in the external oblique muscle in response to graded colorectal distension. * $P < 0.05$, ** $P < 0.01$ vs Normal group, # $P < 0.05$, ## $P < 0.01$ vs D-IBS group. Data are presented as mean \pm SEM ($n=6$).

Abbreviations: AWR, abdominal withdrawal reflex; AUC, area under the curve; EMG, electromyography.

group (GFAP: LSD test, $P = 0.007$; S100 β : LSD test, $P = 0.000$) and decreased IOD in the TXYF group compared to the D-IBS group (GFAP: LSD test, $P = 0.023$; S100 β : LSD test, $P = 0.001$) (Figure 5C and D).

Effect of TXYF on the NGF/TrkA Level and NGF Release

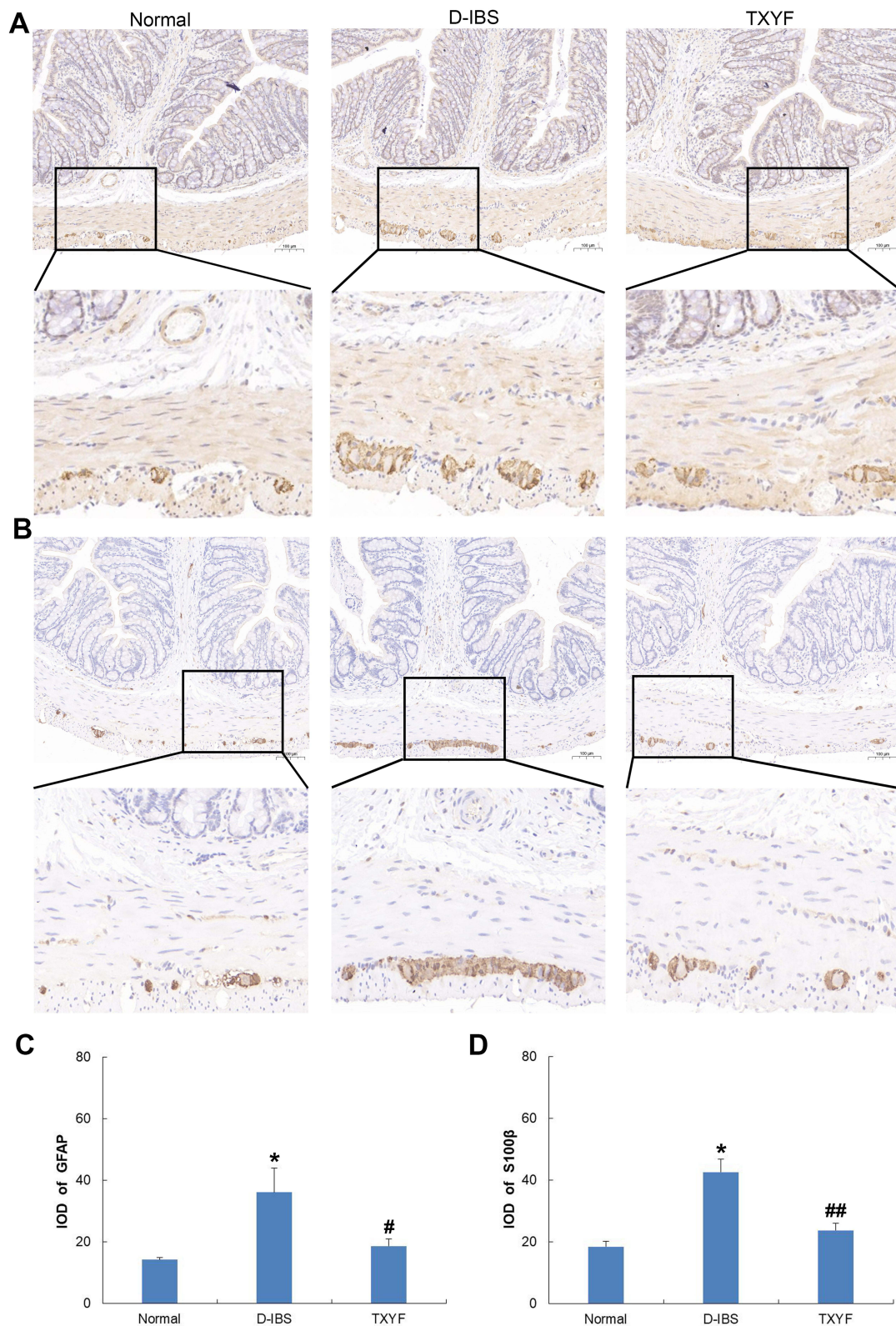
The D-IBS group showed increased levels of NGF and TrkA compared with the Normal group (NGF: LSD test, $P = 0.012$; TrkA: LSD test, $P = 0.002$). After treatment with TXYF, NGF and TrkA levels were significantly lower in the TXYF group than in the D-IBS group (NGF, LSD test, $P = 0.002$; TrkA, LSD test, $P = 0.020$) (Figure 6A and B).

In the ex vivo experiment, the level of NGF released increased in the D-IBS group compared to that in the Normal group (LSD test, $P = 0.029$). After treatment with TXYF, the release of NGF was significantly decreased in the TXYF group compared with that in the D-IBS group (LSD test, $P = 0.002$) (Figure 6C). There were no significant differences among the three groups after pretreatment with the EGC inhibitor DL-fluorocitrate (ANOVA, $P = 0.104$) (Figure 6D).

Effect of TXYF on the Ultrastructure and Synaptic Plasticity of ENS

Images of the ENS under a transmission electron microscope in the Normal, D-IBS, and TXYF groups are shown in Figure 7. In the D-IBS group, the nerve arrangement was denser and more irregular, the spaces between them were reduced, and more synaptic vesicles were present. In the Normal and TXYF groups, nerve arrangement was regular, the spaces between each nerve changed, and the number of synaptic vesicles decreased.

SYN and PSD-95 are involved in synaptic plasticity. Images of SYN (Figure 8A) and PSD-95 (Figure 8B) under a light microscope in the Normal, D-IBS, and TXYF groups. Strong positive particle expression of SYN and PSD-95 was observed, mainly in the myenteric plexus, and a small amount of expression was also found in the submucosal plexus.



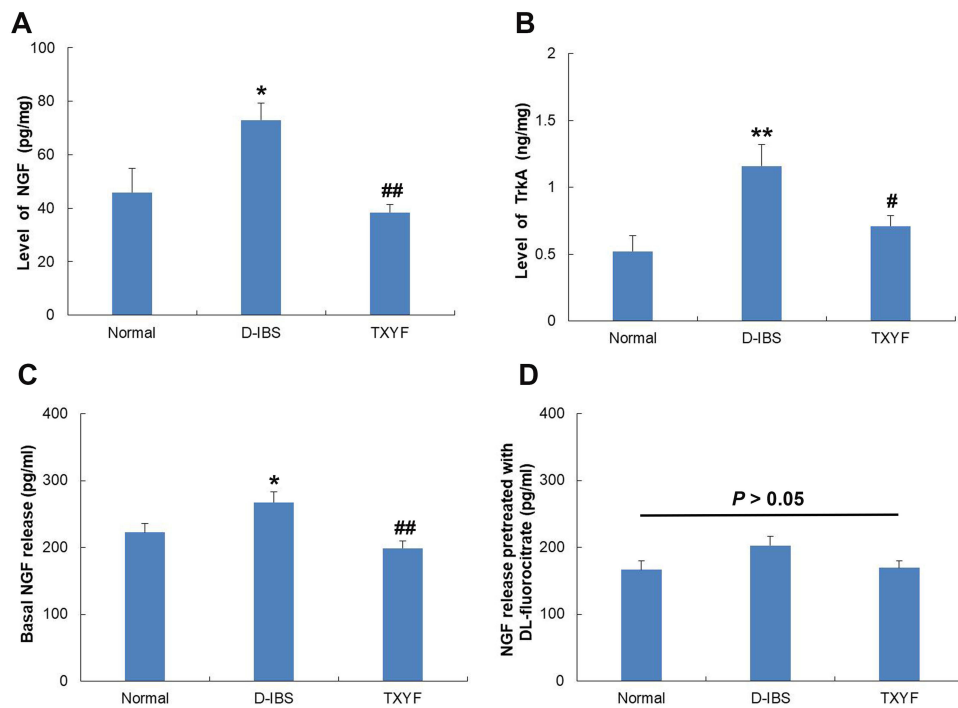


Figure 6 Effect of TXYF on NGF/TrkA level and NGF release in the colon. **(A)** Level of NGF. **(B)** Level of TrkA. **(C)** Basal NGF release. **(D)** NGF release pretreated with EGC inhibitor DL-fluorocitrate. * $P < 0.05$, ** $P < 0.01$ vs Normal group, # $P < 0.05$, ## $P < 0.01$ vs D-IBS group. Data are presented as mean \pm SEM (n=6).

Abbreviations: NGF, nerve growth factor; EGC, enteric glial cell.

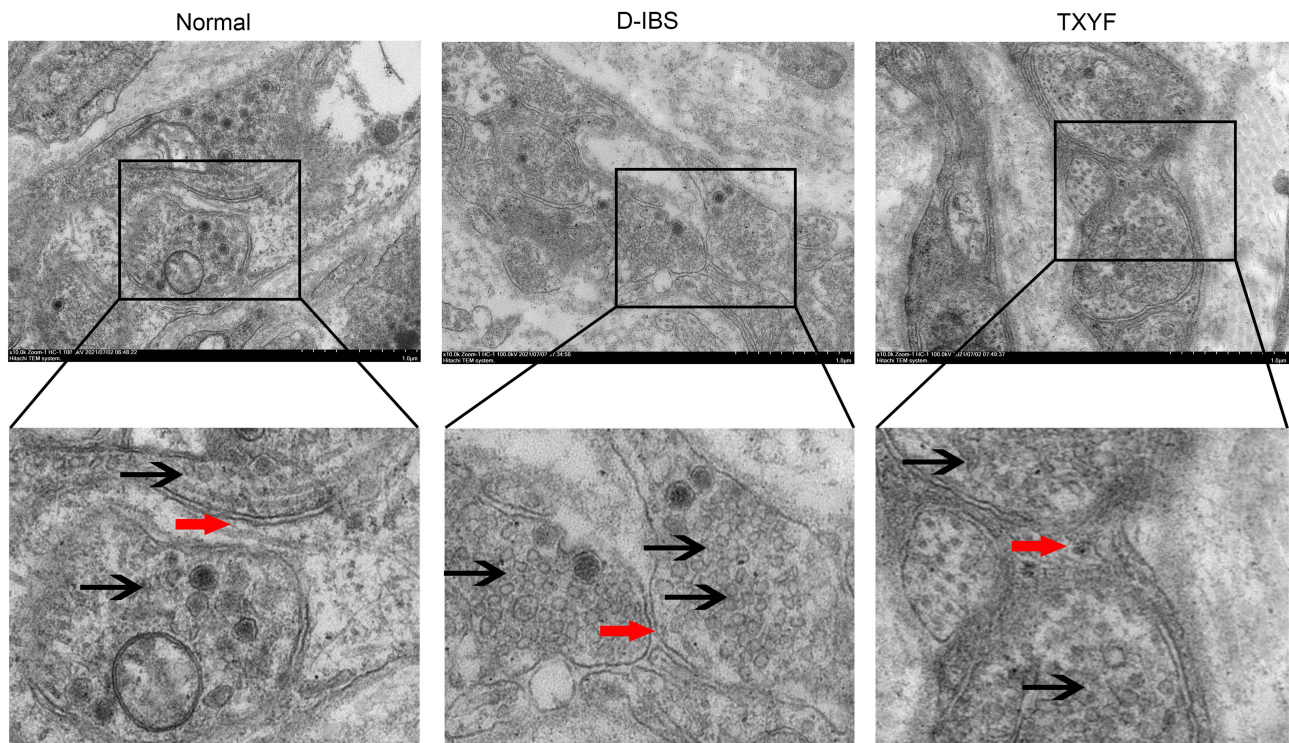


Figure 7 Effect of TXYF on the ultrastructure of ENS in the colon (Scale bar 1.0 μ m). Black arrows indicated synaptic vesicles; red arrows indicated the spaces between each nerve. **Abbreviations:** ENS, enteric nervous system.

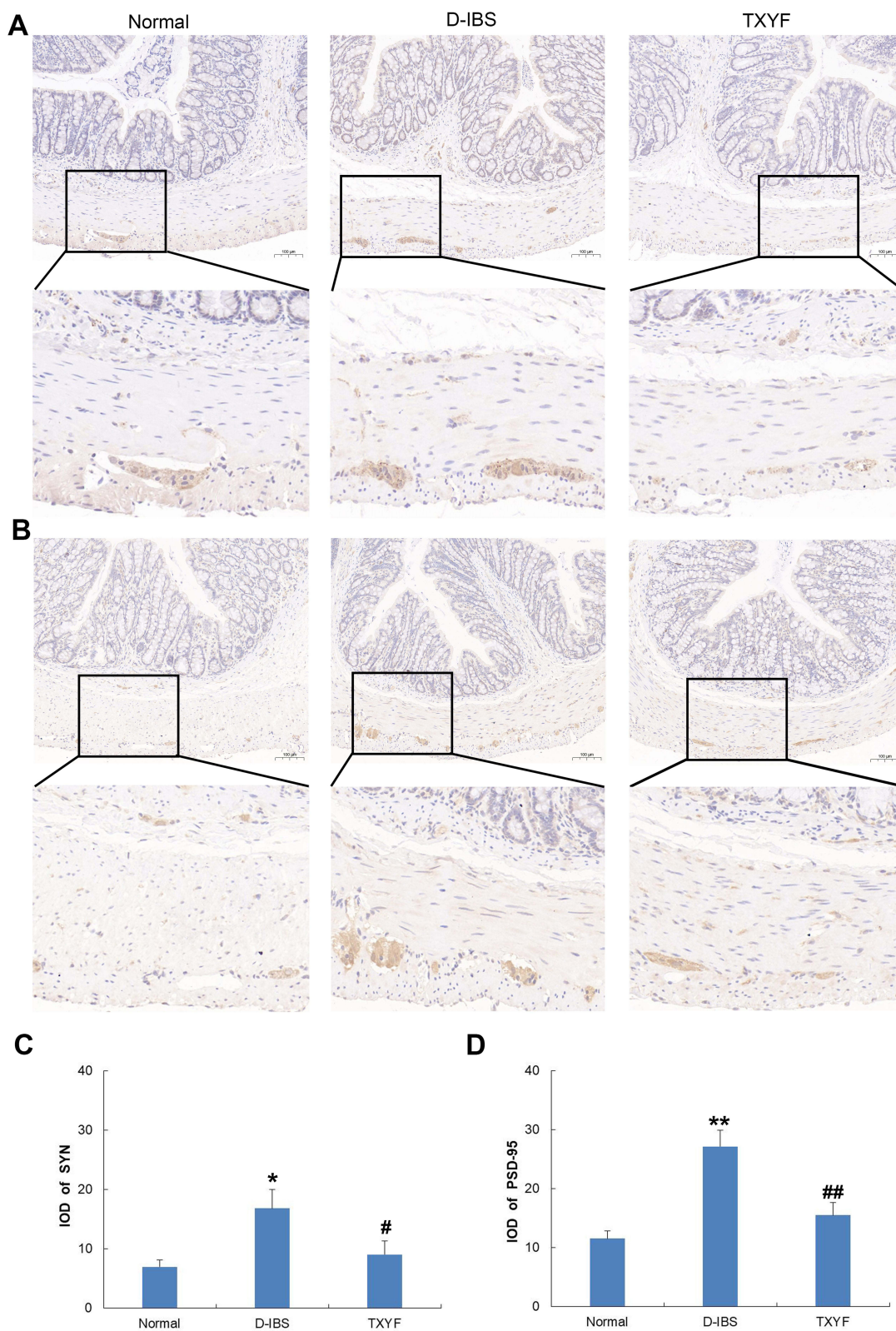


Figure 8 Effect of TXYF on the expression of synaptophysin (SYN) and postsynaptic density-95 (PSD-95) in the colon. **(A)** Immunohistochemical staining of SYN. **(B)** Immunohistochemical staining of PSD-95. (Scale bar 100 μ m). **(C)** Integrated optical density (IOD) of SYN in the colon. **(D)** Integrated optical density (IOD) of PSD-95 in the colon. * $P < 0.05$, ** $P < 0.01$ vs Normal group, # $P < 0.05$, ## $P < 0.01$ vs D-IBS group. Data are presented as mean \pm SEM (n=5).

Abbreviations: SYN, synaptophysin; PSD-95, postsynaptic density-95; IOD, integrated optical density.

The D-IBS group showed increased IOD compared with the Normal group (SYN: LSD test, $P = 0.012$; PSD-95: LSD test, $P = 0.000$), after treatment with TXYF, the IOD significantly decreased in the TXYF group compared with the D-IBS group (SYN: LSD test, $P = 0.038$; PSD-95: LSD test, $P = 0.002$) (Figure 8C and D).

Effect of TXYF on the Glutamate Pathway

The D-IBS group showed increased levels of glutamate and mRNA expression of AMPAR1, NMDAR1, and NMDAR2B compared with the Normal group (glutamate: LSD test, $P = 0.020$; AMPAR1: LSD test, $P = 0.017$; NMDAR1: LSD test, $P = 0.019$; NMDAR2B: LSD test, $P = 0.016$). After treatment with TXYF, the levels of glutamate and mRNA expression of AMPAR1, NMDAR1, and NMDAR2B decreased in the TXYF group compared to the D-IBS group (glutamate: LSD test, $P = 0.006$; AMPAR1: LSD test, $P = 0.034$; NMDAR1: LSD test, $P = 0.044$; NMDAR2B: LSD test, $P = 0.027$) (Figure 9).

Discussion

In this study, a D-IBS rat model was established by the method of neonatal maternal separation and restraint stress. The results showed that TXYF could relieve visceral hypersensitivity, meanwhile, reduce the colonic level of GFAP, calcium-binding protein S100 β , NGF and TrkA, down-regulate the colonic expression of SYN and PSD-95, and lower the level of glutamate and colonic mRNA expression of AMPAR1, NMDAR1 and NMDAR2B in D-IBS rats. In an ex vivo experiment, TXYF reduced colonic NGF release, and this effect was inhibited by an EGC inhibitor. These results suggest that TXYF alleviates intestinal hypersensitivity in D-IBS rats, which may be achieved by inhibiting EGC activation and the NGF/TrkA signaling pathway, thereby affecting neural synaptic plasticity. A model diagram of the TXYF pathway for D-IBS is shown in Figure 10.

TXYF Attenuated Visceral Hypersensitivity in D-IBS Rats

D-IBS is a functional disorder that typically results in abdominal pain and diarrhea. Although the exact pathological mechanisms of D-IBS remain unclear, visceral hypersensitivity has been accepted as a conceivable mechanism.

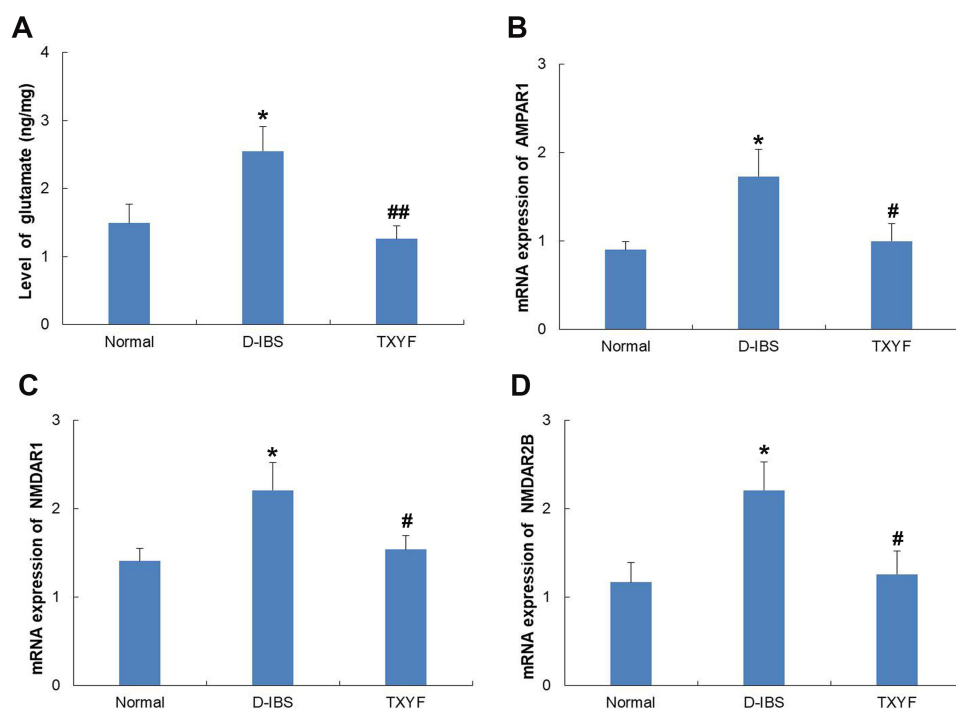


Figure 9 Effect of TXYF on the glutamate pathway in colon. (A) Level of glutamate; (B) Relative mRNA expression of AMPAR1; (C) Relative mRNA expression of NMDAR1; (D) Relative mRNA expression of NMDAR2B. * $P < 0.05$ vs Normal group, # $P < 0.05$, ## $P < 0.01$ vs D-IBS group. Data are presented as mean \pm SEM ($n=6$).
Abbreviations: AMPAR, α -amino-3-hydroxy-5-methyl-4-isoxazole-propionic acid receptor; NMDAR, N-methyl-D-aspartate receptor.

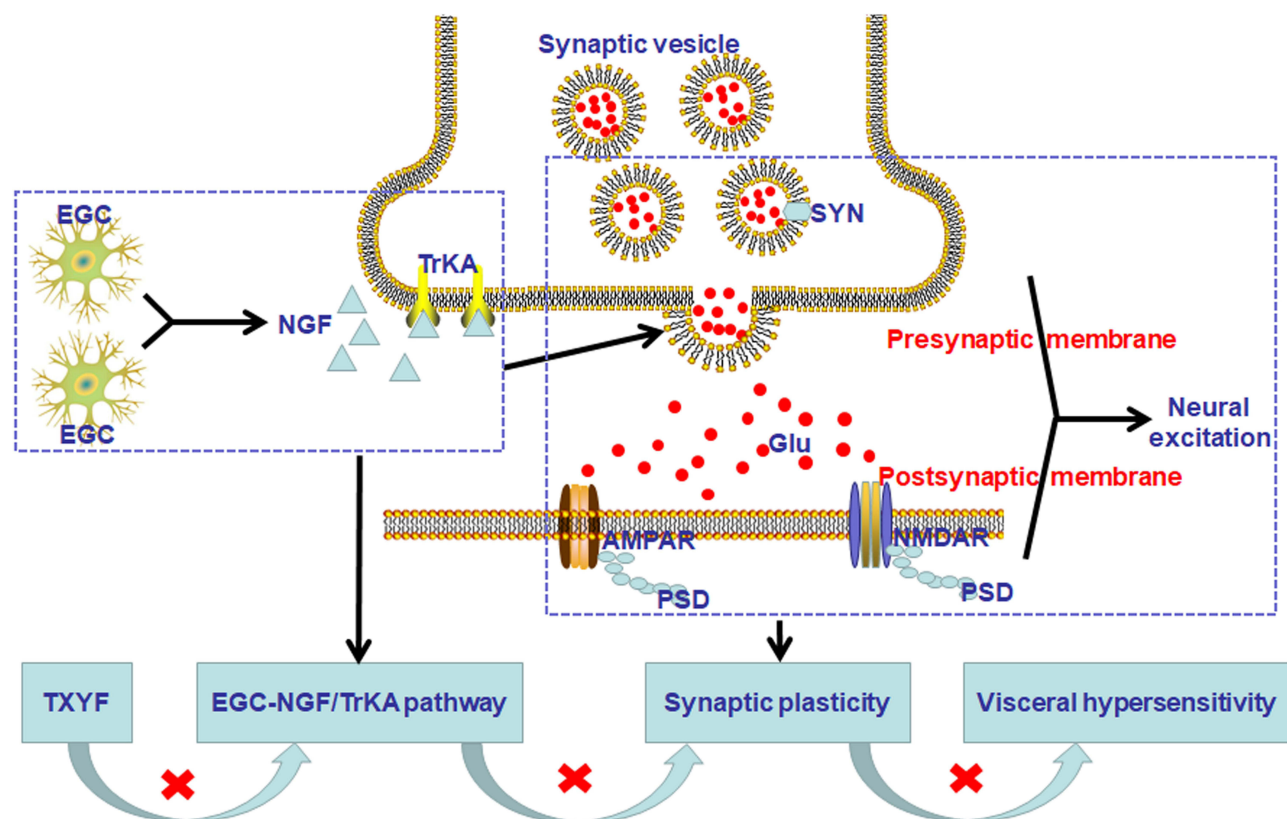


Figure 10 The model diagram of TXYP mechanism pathway on D-IBS. TXYP could inhibit EGC activation and NGF/TrkA signaling pathway, then affect neural synaptic plasticity to alleviate intestinal hypersensitivity in D-IBS.

Abbreviations: EGC, enteric glial cells; NGF, nerve growth factor; SYN, synaptophysin; PSD, postsynaptic density; Glu, glutamate; AMPAR, α -amino-3-hydroxy-5-methyl-4-isoxazole-propionic acid receptor; NMDAR, N-methyl-D-aspartate receptor.

A previous retrospective analysis had been demonstrated that in 407 IBS patients, 36% of patients showed allodynia and 22% of patients showed hyperalgesia, which were associated with severity of IBS symptoms.²¹ Besides, large amounts of animal experiments imitating the IBS-like process showed visceral hypersensitivity participated in IBS.²²

In TCM, TXYP has been recognized as an effective prescription in treating liver depression and spleen deficiency type of diarrhea with pain. It has been first recorded by Zhu Danxi, a doctor in the Yuan Dynasty, which is composed of four herbs (Rhizoma Atractylodis Macrocephalae, Radix Paeoniae Alba, Pericarpium Citri Reticulatae and Radix Saposhnikoviae) and plays the role of soothing liver and strengthening spleen.²³ In current times, a series of clinic-based trials have demonstrated that TXYP is obviously effective in the treatment of D-IBS patients. A systematic review and meta-analysis conducted in 2022 has included a total of 985 D-IBS patients from 11 randomized controlled trials and the analysis results showed that TXYP was superior to western medication or placebo in the improvement of stool consistency, stool frequency, abdominal pain and the quality of life, as well as in relieving anxiety.²⁴

In our study, we validated that the visceral hypersensitivity was also present in D-IBS rats which was quantified by the strengthening trends of AWR score and EMG response. TXYP significantly reversed this elevation, which is in agreement with the previous observations.²⁵

TXYP Inhibited the Activity of EGC and NGF/TrkA Pathway in D-IBS Rats

Intestinal hypersensitivity has been associated with abnormal neuromodulation of the gut-brain axis, in which the ENS played an irreplaceable role.²⁶ As the structure and function of the central nervous system, ENS has been thought of as the “brain” in the gut, which comprised the neurons, ganglia, and nerve fibers.²⁷ Besides, as an important nutritive and supporting cell of ENS, the role of EGCs in the neuromodulation has been paid more and more attention. EGCs are mainly distributed in the submucosal and myenteric plexus.²⁸ GFAP and calcium-binding protein S100 β express in activated EGCs, which are reliable

molecular biomarkers of EGCs.²⁹ A previous study used the method of maternal separation and water avoidance to establish a visceral hypersensitivity rat model and found EGCs activation and increased GFAP expression in the model rats, suggesting that the activation of EGCs plays a role in intestinal hypersensitivity.³⁰ Fujikawa et al³¹ found that the number of GFAP-positive EGCs overlapping neurons in the myenteric plexus increased significantly in a rat model of maternal separation combined with acute stress. Moreover, in the model group, the longitudinal smooth muscle contraction intensity of the colon increased, and the contractile intensity was significantly inhibited by the EGC inhibitor, suggesting that EGC is closely related to the regulation of neural electrical activity.

EGC is similar to astrocytes in the central nervous system and comprises many secretory vesicles that can secrete neurotrophic factors. Among these, NGF was the first one discovered.¹¹ In recent years, a large number of studies have reported that NGF can bind to the high-affinity TrkA receptor to participate in the regulation of visceral sensitivity. An experimental animal study showed that in D-IBS model rats, colonic protein expression of NGF and TrkA increased, which was thought to be associated with visceral sensitivity.³² A report by Chen et al³³ reached a similar conclusion in a rat model of post-inflammatory rectal hypersensitivity.

Based on the above research, we explored changes in the EGC-NGF/TrkA pathway in D-IBS and found that the immunohistochemical expression of GFAP and calcium-binding protein S100 β was mainly expressed in the myenteric plexus, and a small amount was found in the submucosal plexus. The immunohistochemical expression of GFAP and S100 β was up-regulated, the contents of NGF and TrkA increased in the colon of D-IBS rats, and TXYF had an inhibitory effect on them. To further demonstrate the relationship between EGC and NGF, we measured NGF release. It has been found that NGF release increased in D-IBS rats, TXYF could reduce NGF release. After pretreatment with the EGC inhibitor DL-fluorocitrate, NGF release decreased in each group, and no difference was found among the three groups, demonstrating that NGF originating from EGCs plays a significant role in the effect of TXYF on visceral sensitivity.

TXYF Improved Neural Synaptic Plasticity in D-IBS Rats

Studies have proved that NGF receptors are found in the nerves and immune cells. On the one hand, NGF binding to receptors can promote neuronal phosphorylation and activate different secondary messengers, then further achieve pain-related signal transduction. On the other hand, NGF receptors can activate the immune response and promote the release of inflammatory cytokines, such as interleukin and TNF, which then act on nerve fiber endings.^{34,35} In addition, in recent years, studies have directly pointed out that intestinal hypersensitivity induced by NGF is related to synaptic plasticity. A previous study found that colonic synaptic density, SYN, and PSD-95 expression were increased in rats with intestinal hypersensitivity induced by water avoidance stress. In further *in vitro* experiments the *c-fos* expression in myenteric plexus incubated with colonic mucosal supernatant of model group rats increased and NGF antibody had a significant inhibitory effect on it, suggesting that NGF-mediated synaptic plasticity plays a certain role in intestinal hypersensitivity.¹⁹ The process of synaptic plasticity involved multiple factors as SYN, PSD, calbindin-28K, *c-fos*, the immediate early genes and activity-regulated cytoskeleton-associated protein (*arc*).³⁶ In our study, we mainly discussed the role of SYN and PSD in D-IBS. SYN was involved in the formation of synaptic vesicles and exocytosis.³⁷ PSD has been known as the key postsynaptic substance participating in the transduction and integration of neural signals in which PSD-95, as an important component of PSD, has been confirmed to be associated with the formation and maintenance of synaptic junctions.³⁸ It was found that in D-IBS rats, under the transmission electron microscopy, the denser nerve arrangement and more synaptic vesicles were found indicating that there may be more signal transduction. Using immunohistochemistry, we examined the up-regulated expression of SYN and PSD-95. Moreover, we found that the positive particle expression of SYN and PSD-95 was concentrated in the myenteric plexus, similar to GFAP and S100 β , which facilitated the interaction between EGCs and ENS. All of the above findings indicate that neural synaptic plasticity participated in intestinal hypersensitivity in D-IBS rats. Furthermore, we found that TXYF reduced the expression of SYN and PSD-95, indicating that relief of visceral hypersensitivity by TXYF may be achieved by improving neural synaptic plasticity.

PSD-95, a membrane-associated guanylate kinase family member, is a unique protein in glutamatergic postsynaptic membranes. PSD-95 can connect with the glutamate receptors N-methyl-D-aspartate receptor (NMDAR) and α -amino-3-hydroxy-5-methyl-4-isoxazole-propionic acid receptor (AMPA) to participate in signal transduction and maintain the stability of the postsynaptic membrane.³⁹ For the glutamate receptors subtypes, AMPAR1, NMDAR1 and NMDAR2B have

been demonstrated playing an important role in chronic pain or visceral hypersensitivity.⁴⁰ In AMPAR subtypes, AMPAR1 whether in the central system or the peripheral organs played an important role in synaptic plasticity related to chronic pain.^{41,42} Besides, NMDAR1 and NMDAR2 have been recognized as two functional subunits of NMDAR. It was reported in 2006 that NMDAR1 expression elevated selectively in the myenteric plexus of colitis rats, which was related with chronic visceral hypersensitivity.⁴³ NMDAR2B has strong affinity with glutamate, a clinical report demonstrated that higher colonic expression of NMDAR2B has been found in D-IBS patients, which positively correlated with the scores of the IBS Symptom Severity Scale.⁴⁴ Based on the above, in our study, the glutamate and three receptor subtypes were detected, and it has been found that the level of glutamate and mRNA expression of AMPAR1, NMDAR1 and NMDAR2B was up-regulated in D-IBS rats and TXYF could reduce the high level, which indicated glutamate and specific receptors participated in the regulation of TXYF for synaptic plasticity.

Conclusion

TXYF can relieve visceral hypersensitivity in rats with IBS-D, possibly by improving neural synaptic plasticity through inhibition of the activity of EGCs and the NGF/TrkA signaling pathway. In addition, the myenteric plexus, an important target of TXYF, was discovered, providing more ideas for further research.

Funding

This work was funded by the National Natural Science Foundation of China (No. 82004266).

Disclosure

The authors declare that there are no conflicts of interest in this work.

References

1. Mearin F, Lacy BE, Chang L, et al. Bowel disorders. *Gastroenterology*. 2016;150(16):1393–1407. doi:10.1053/j.gastro.2016.02.031
2. Oka P, Parr H, Barberio B, Black CJ, Savarino EV, Ford AC. Global prevalence of irritable bowel syndrome according to Rome III or IV criteria: a systematic review and meta-analysis. *Lancet Gastroenterol Hepatol*. 2020;5(10):908–917. doi:10.1016/S2468-1253(20)30217-X
3. Sperber AD, Bangdiwala SI, Drossman DA, et al. Worldwide prevalence and burden of functional gastrointestinal disorders, results of Rome foundation global study. *Gastroenterology*. 2021;160(1):99–114.e3. doi:10.1053/j.gastro.2020.04.014
4. Liu J, Hou X. A review of the irritable bowel syndrome investigation on epidemiology, pathogenesis and pathophysiology in China. *J Gastroenterol Hepatol*. 2011;26(Suppl s3):88–93. doi:10.1111/j.1440-1746.2011.06641.x
5. Bonetto S, Fagoonee S, Battaglia E, Grassini M, Saracco GM, Pellicano R. Recent advances in the treatment of irritable bowel syndrome. *Pol Arch Intern Med*. 2021;131(7–8):709–715. doi:10.20452/pamw.16067
6. Xu W, Zhang Z, Lu Y, Li M, Li J, Tao W. Traditional Chinese medicine Tongxie Yaofang treating irritable bowel syndrome with diarrhea and type 2 diabetes mellitus in rats with liver-depression and spleen-deficiency: a preliminary study. *Front Nutr*. 2022;9:968930. doi:10.3389/fnut.2022.968930
7. Chen X, Yu X, Shi Y, Shen H. Overview of systematic evaluation of efficacy of Tongxie Yaofang in treating diarrhea-predominant irritable bowel syndrome. *Ann Palliat Med*. 2021;10(8):9223–9232. doi:10.21037/apm-21-1612
8. Hadjivasilis A, Tsioutis C, Michalinos A, Ntourakis D, Christodoulou DK, Agouridis AP. New insights into irritable bowel syndrome: pathophysiology to treatment. *Ann Gastroenterol*. 2019;32(6):554–564. doi:10.20524/aog.2019.0428
9. Hou Q, Huang Y, Zhu Z, et al. Tong-Xie-Yao-Fang improves intestinal permeability in diarrhoea-predominant irritable bowel syndrome rats by inhibiting the NF- κ B and notch signalling pathways. *BMC Complement Altern Med*. 2019;19(1):337. doi:10.1186/s12906-019-2749-4
10. Yang X, Sheng L, Guan Y, Qian W, Hou X. Synaptic plasticity: the new explanation of visceral hypersensitivity in rats with *Trichinella spiralis* infection? *Dig Dis Sci*. 2009;54(5):937–946. doi:10.1007/s10620-008-0444-2
11. López-Pérez AE, Nurgali K, Abalo R. Painful neurotrophins and their role in visceral pain. *Behav Pharmacol*. 2018;29(2–3):120–139. doi:10.1097/FBP.0000000000000386
12. Morales-Soto W, Gulbransen BD. Enteric glia: a new player in abdominal pain. *Cell Mol Gastroenterol Hepatol*. 2019;7(2):433–445. doi:10.1016/j.jcmgh.2018.11.005
13. Arifin WN, Zahiruddin WM. Sample size calculation in animal studies using resource equation approach. *Malays J Med Sci*. 2017;24(5):101–105. doi:10.21315/mjms2017.24.5.11
14. Percie du Sert N, Hurst V, Ahluwalia A, et al. The ARRIVE guidelines 2.0: updated guidelines for reporting animal research. *Br J Pharmacol*. 2020;177(16):3617–3624. doi:10.1111/bph.15193
15. Wu H, Zhan K, Rao K, et al. Comparison of five diarrhea-predominant irritable bowel syndrome (IBS-D) rat models in the brain-gut-microbiota axis. *Biomed Pharmacother*. 2022;149:112811. doi:10.1016/j.biopha.2022.112811
16. Li L, Cui H, Li T, et al. Synergistic effect of berberine-based Chinese medicine assembled nanostructures on diarrhea-predominant irritable bowel syndrome in vivo. *Front Pharmacol*. 2020;11:1210. doi:10.3389/fphar.2020.01210
17. Qi DB, Zhang SH, Zhang YH, Wu SQ, Li WM. A rat model for studying electroacupuncture analgesia on acute visceral hyperalgesia. *Exp Anim*. 2018;67(1):51–61. doi:10.1538/expanim.17-0063

18. Chen L, Wang Y, Li S, Zhou W, Sun L. High expression of NDRG3 in osteoarthritis patients. *Arthroplasty*. 2021;3(1):1. doi:10.1186/s42836-020-00064-2
19. Zhang L, Song J, Bai T, Wang R, Hou X. Sustained pain hypersensitivity in the stressed colon: role of mast cell-derived nerve growth factor-mediated enteric synaptic plasticity. *Neurogastroenterol Motil*. 2018;30(9):e13430. doi:10.1111/nmo.13430
20. Nasser Y, Fernandez E, Keenan CM, et al. Role of enteric glia in intestinal physiology: effects of the gliotoxin fluorocitrate on motor and secretory function. *Am J Physiol Gastrointest Liver Physiol*. 2006;291(5):G912–927. doi:10.1152/ajpgi.00067.2006
21. Simrén M, Törnblom G, Palsson OS, Van Oudenhove L, Whitehead WE, Tack J. Cumulative effects of psychologic distress, visceral hypersensitivity, and abnormal transit on patient-reported outcomes in irritable bowel syndrome. *Gastroenterology*. 2019;157(2):391–402.e2. doi:10.1053/j.gastro.2019.04.019
22. Zhao Y, Jiang H-L, Shi Y, et al. Electroacupuncture alleviates visceral hypersensitivity in IBS-D rats by inhibiting EGCs Activity through regulating BDNF/TrkB signaling pathway. *Evid Based Complement Alternat Med*. 2022;2022:2497430. doi:10.1155/2022/2497430
23. Deng ZJ. *Formulas of Chinese Medicine*. Beijing, China: Chinese Press of Traditional Chinese Medicine; 2010.
24. Liang SB, Cao HJ, Kong LY, et al. Systematic review and meta-analysis of Chinese herbal formula Tongxie Yaofang for diarrhea-predominant irritable bowel syndrome: evidence for clinical practice and future trials. *Front Pharmacol*. 2022;13:904657. doi:10.3389/fphar.2022.904657
25. Lin Y, Ding Y, B L, Liu N. Effect of Tongxieyaofang decoction on colonic mucosal protein expression profiles in rats with visceral hypersensitivity. *J Tradit Chin Med*. 2020;40(2):245–252.
26. Aziz MNM, Kumar J, Muhammad Nawawi KN, Raja Ali RA, Mokhtar NM. Irritable bowel syndrome, depression, and neurodegeneration: a bidirectional communication from gut to brain. *Nutrients*. 2021;13(9):3061. doi:10.3390/nu13093061
27. Kulkarni S, Ganz J, Bayrer J, et al. Advances in enteric neurobiology: the “Brain” in the gut in health and disease. *J Neurosci*. 2018;38(44):9346–9354. doi:10.1523/JNEUROSCI.1663-18.2018
28. Grubišić V, Gulbransen BD. Enteric glia: the most alimentary of all glia. *J Physiol*. 2017;595(2):557–570. doi:10.1113/JP271021
29. Grundmann D, Loris E, Maas-Omlor S, et al. Enteric glia: S100, GFAP, and beyond. *Anat Rec*. 2019;302(8):1333–1344. doi:10.1002/ar.24128
30. Xu S, Qin B, Shi A, Zhao J, Guo X, Dong L. Oxytocin inhibited stress induced visceral hypersensitivity, enteric glial cells activation, and release of proinflammatory cytokines in maternally separated rats. *Eur J Pharmacol*. 2018;818:578–584. doi:10.1016/j.ejphar.2017.11.018
31. Fujikawa Y, Tominaga K, Tanaka F, et al. Enteric glial cells are associated with stress-induced colonic hyper-contraction in maternally separated rats. *Neurogastroenterol Motil*. 2015;27(7):1010–1023. doi:10.1111/nmo.12577
32. Yang YC, Zhou ZX, Xue T, et al. Effect of electroacupuncture on visceral sensitivity and colonic NGF, TrkA, TRPV1 expression in IBS-D rats. *Zhongguo Zhen Jiu*. 2022;42(12):1395–1402. doi:10.13703/j.0255-2930.20220130-0005
33. Chen Y, Cheng J, Zhang Y, Chen JDZ, Seralu FM. Electroacupuncture at ST36 relieves visceral hypersensitivity via the NGF/TrkA/TRPV1 peripheral afferent pathway in a rodent model of post-inflammation rectal hypersensitivity. *J Inflamm Res*. 2021;14:325–339. doi:10.2147/JIR.S285146
34. Hirose M, Kuroda Y, Murata E. NGF/TrkA signaling as a therapeutic target for pain. *Pain Pract*. 2016;16(2):175–182. doi:10.1111/papr.12342
35. Thacker MA, Clark AK, Marchand F, et al. Pathophysiology of peripheral neuropathic pain: immune cells and molecules. *Anesth Analg*. 2007;105(3):838–847. doi:10.1213/01.ane.0000275190.42912.37
36. Zhang L, Wang R, Bai T, et al. EphrinB2/ephB2-mediated myenteric synaptic plasticity: mechanisms underlying the persistent muscle hypercontractility and pain in postinfectious IBS. *FASEB J*. 2019;33(12):13644–13659. doi:10.1096/fj.201901192R
37. Kokotos AC, Harper CB, Marland JRK, Smillie KJ, Cousin MA, Gordon SL. Synaptophysin sustains presynaptic performance by preserving vesicular synaptobrevin-II levels. *J Neurochem*. 2019;151(1):28–37. doi:10.1111/jnc.14797
38. Levy AM, Gomez-Puertas P, Tümer Z. Neurodevelopmental disorders associated with PSD-95 and its interaction partners. *Int J Mol Sci*. 2022;23(8):4390. doi:10.3390/ijms23084390
39. Chen X, Levy JM, Hou A, et al. PSD-95 family MAGUKs are essential for AMPA and NMDA receptor complexes at the postsynaptic density. *Proc Natl Acad Sci U S A*. 2015;112(50):E6983–E6992. doi:10.1073/pnas.1517045112
40. Baj A, Moro E, Bistoletti M, Orlandi V, Crema F, Giaroni C. Glutamatergic signaling along the microbiota-gut-brain axis. *Int J Mol Sci*. 2019;20(6):1482. doi:10.3390/ijms20061482
41. Bai Y, Chen YB, Qiu XT, et al. Nucleus tractus solitarius mediates hyperalgesia induced by chronic pancreatitis in rats. *World J Gastroenterol*. 2019;25(40):6077–6093. doi:10.3748/wjg.v25.i40.6077
42. Xu G, Li T, Huang Y. The effects of intraoperative hypothermia on postoperative cognitive function in the rat hippocampus and its possible mechanisms. *Brain Sci*. 2022;12(1):96. doi:10.3390/brainsci12010096
43. Zhou Q, Caudle RM, Price DD, Valle-Pinero AY D, Verne GN. Selective up-regulation of NMDA-NR1 receptor expression in myenteric plexus after TNBS induced colitis in rats. *Mol Pain*. 2006;2:3. doi:10.1186/1744-8069-2-3
44. Li P, Zheng J, Bai Y, et al. Characterization of kynurenine pathway in patients with diarrhea-predominant irritable bowel syndrome. *Eur J Histochem*. 2020;64(s2):3132. doi:10.4081/ejh.2020.3132